

### 3.5.4 ICRS Centre

#### Introduction

The IAU has charged the IERS with the responsibility of monitoring the International Celestial Reference System (ICRS), maintaining its current realization, the International Celestial Reference Frame (ICRF), and maintaining and improving the links with other celestial reference frames. Starting in 2001, these activities have been run jointly by the ICRS Centre (Observatoire de Paris and US Naval Observatory) of the IERS and the International VLBI Service for Geodesy and Astrometry (IVS), in coordination with the IAU. The present report was jointly prepared by the Paris Observatory and US Naval Observatory components of the ICRS Centre. The ICRS Centre web site (<<http://hpiers.obspm.fr/icrs-pc>>) provides information on the characterization and construction of the ICRF (radio source nomenclature, physical characteristics of radio sources, astrometric behaviour of a set of sources, radio source structure). This information is also available by anonymous ftp (<[hpiers.obspm.fr/icrs-pc](ftp://hpiers.obspm.fr/icrs-pc)>), and on request to the ICRS Centre ([icrspc@hpopa.obspm.fr](mailto:icrspc@hpopa.obspm.fr)).

#### Maintenance and extension of the ICRF

In the framework of the validation of individual VLBI references frames, individual celestial reference frames obtained in 2008 by three laboratories have been compared to ICRF-Ext.2 (Fey et al., 2004).

#### The reference frames analyzed

The individual frame RSC (BKGI) 08 R 03 elaborated at the Federal Agency for Cartography and Geodesy and the Geodetic and Geoinformation Institute of the University of Bonn (Germany) has been evaluated using CALC 10.0 / SOLVE release 2007.10.04. The celestial reference frame has been oriented by a no-net-rotation constraint imposed to the positions of the 212 defining sources as in ICRF-Ext.1 (IERS 1999). The a priori precession and nutation models are IERS 2003. Troposphere gradients have been adjusted in the solution. The time span of the observations is January 1984 – November 2008. VMF1 mapping function has been applied for the troposphere modeling.

RSC (IAA) 08 R 01 is the extragalactic frame produced by the Institute of Applied Astronomy in Saint Petersburg, Russia with the QUASAR software. The observations range in the period August 1979 – October 2008. The celestial frame has been oriented by a no-net-rotation imposed to the positions of 212 defining sources in ICRF-Ext.2. The a priori precession and nutation models are both IAU 2000. Troposphere gradients have been adjusted in the solution.

The RSC (OPA) 08 R 01 frame was obtained at the Paris Observatory analysis centre with the CALC 10.0 / Solve 2008.07.31 software. The a priori models are IERS 2003 for the precession and IAU 2000 for the nutation. A no-net-rotation constraint is applied to the 247 stable sources of Feissel-Vernier et al. (2006). The VLBI observation analyzed span over the period January 1984 – December 2008 and the NMF mapping function has been applied for the troposphere modeling. Troposphere gradients have been adjusted in the solution.

*Table 1: Individual VLBI celestial reference frames analyzed.  $n$  is the number of sources,  $m$  is the median of the coordinate uncertainties. Unit: mas.*

Frame	Tot.	Defining		Candidate		Other		New		Additional		dec (°)
	N	n	m	n	m	n	m	n	m	N	m	
RSC (BKGI) 08 R 03	1868	209	0.04	225	0.04	101	0.02	84	0.09	1249	0.41	-81;+89
RSC (IAA) 08 R 01	1037	212	0.05	285	0.09	102	0.03	109	0.20	389	0.54	-85;+84
RSC (OPA) 08 R 01	603	209	0.06	102	0.07	98	0.03	50	0.11	44	0.18	-81;+84

Positions and velocities of stations have been estimated as global parameters for the three frames with a no-net-translation and a no-net-rotation constraints applied on 26 VTRF2005 stations for the BKGI, 11 VTRF2005 stations for the IAA, 35 ITRF2000 stations for the OPA.

The characteristics of the analyzed frames are given in Table 1. Five categories of sources appear in the table: *defining*, *candidate* and *other* correspond to the classification of ICRF sources (Ma et al., 1998); *new* refers to the sources added in ICRF-Ext.2; *additional* represents sources observed in VLBI programs and not present in ICRF-Ext.2. The values of the median of the coordinate uncertainties indicate that all frames are of similar quality.

#### Comparison of individual celestial frames to ICRF-Ext.2

The catalogues listed in Table 1 have been compared to ICRF-Ext.2. The algorithm of comparison revised last year was used. The coordinate differences between two frames are modeled by a global rotation of the axes, represented by the angles  $A_1$ ,  $A_2$ ,  $A_3$ , and by a deformation represented by one parameter:  $dz$ , which is a bias between the principal plane of the frame relative to that of ICRF-Ext.2. In the fitting used until 2006 slopes in right ascension and declination were modeled; as these deformation parameters proved to be negligible over some years of comparison, they have been removed from the model. Parameter  $dz$  is equivalent to the former  $B_\delta$ .

$$\Delta\alpha = A_1 \operatorname{tg} \bar{\delta} \cos \alpha + A_2 \operatorname{tg} \bar{\delta} \sin \alpha - A_3$$

$$\Delta\bar{\delta} = -A_1 \sin \alpha + A_2 \cos \alpha + dz$$

Under the hypothesis that ICRF-Ext.2 is free from deformations, the systematic effects detected in the comparisons should be interpreted as deformations in the individual frames. Defining sources common to each individual frame and ICRF-Ext.2 have been used for the comparisons. The four parameters have been evaluated by a weighted least squares fit; the equations have been weighted using the inverse of the variance of the coordinate differences. The fitted parameters allow the transformation of coordinates in the individual frames into ICRS.

**Results** The results of the comparisons are shown in Table 2 for the values of the transformation parameters and in Figure 1 for the distribution of the postfit residuals.

*Table 2: Transformation parameters between individual catalogues and ICRF-Ext.2. Here, N stands for the number of ICRF defining sources used for fitting the parameters. Unit:  $\mu\text{as}$ .*

Frame	N	$A_1$	$A_2$	$A_3$	Dz
RSC (BKGI) 08 R 03	209	$0 \pm 16$	$-26 \pm 16$	$-14 \pm 17$	$-33 \pm 14$
RSC (IAA) 08 R 01	212	$-11 \pm 19$	$-41 \pm 19$	$-7 \pm 20$	$-18 \pm 17$
RSC (OPA) 08 R 01	209	$-44 \pm 19$	$7 \pm 18$	$-11 \pm 19$	$-16 \pm 16$

The values of the angles  $A_1, A_2, A_3$  in Table 2 show that the individual reference frames realize the axes of the ICRF better than 45  $\mu\text{as}$ , and that they are consistent at the level of their uncertainties. These uncertainties indicate that, after rotation, the inconsistency between the directions of the axes is at most 25  $\mu\text{as}$ . The dz parameter quantifies the bias between the principal plane of each individual frames and that of the ICRS. For the solution computed by BKGI, the bias is significant. In contrast, the principal planes of the OPA and IAA frames are aligned to that of ICRS at the level of 18  $\mu\text{as}$ .

### Investigation of future realizations of the ICRS

The International Celestial Reference System (ICRS), adopted by the International Astronomical Union (IAU) in 1997, forms the underlying basis for all astrometry by defining the reference directions of a quasi-inertial celestial coordinate system that are fixed with respect to the most distant objects in the universe. Since 1 January 1998, the ICRS has been realized by the International Celestial Reference Frame (ICRF) which is based on the radio wavelength astrometric positions of compact extragalactic objects determined by the technique of very long baseline interferometry (VLBI).

### 3.5.4 ICRS Centre

In coordination with the IAU, the task of maintaining the ICRS was given to the International Earth Rotation and Reference System Service (IERS), with the International VLBI Service for Geodesy and Astrometry (IVS) having operational responsibility for the VLBI realization. Significant developments and improvements in geodetic/astrometric VLBI observing and analysis have been made since the initial generation of the ICRF, hereafter ICRF1. Sensitivity of VLBI observing systems to weaker sources and overall data quality have improved significantly due to advances in VLBI receiver and recording systems and due to better observing strategies coordinated by the IVS. The use of newer and more modern radio telescopes, such as the 10 station Very Long Baseline Array (VLBA) of the National Radio Astronomy Observatory, has also greatly improved the sensitivity and quality of recent data. Further, enhanced geophysical modeling and computers with faster processors have allowed significant improvements in data analysis techniques and astrometric position estimation.

With the addition of over fourteen years of new geodetic/astrometric VLBI data taken since ICRF1, we are now better able to select a set of more positionally stable sources, which are more uniformly distributed on the sky and are better able to define the ICRS axes. The additional data also allows us to filter out the most positionally unstable sources, avoiding possible distortion of the frame that might otherwise occur. Further, the large amount of imaging data now available allows us to identify and remove sources with extensive intrinsic structure that could cause potential problems due to temporal structure changes.

At the XXVI meeting of the IAU General Assembly held in Prague, Czech Republic in 2006, an IAU Working Group was established specifically to oversee the generation of a second realization of the International Celestial Reference Frame, hereafter ICRF2. An IERS/IVS Working Group was then established specifically for the purpose of generating ICRF2. This was a truly international effort with Working Group members from numerous countries including the USA, France, Germany, Italy, Russia, Ukraine, Australia, and China.

The end result of the 3-year effort of the IERS/IVS Working Group was ICRF2 (Fey, Gordon and Jacobs, 2009), which contains precise positions of 3414 compact extragalactic sources, more than five times the number as in ICRF1. The ICRF2 has a noise floor of approximately 40 micro-arcseconds, some 5–6 times better than ICRF1, and an axis stability of approximately 10 micro-arcseconds, nearly twice as stable as ICRF1. Alignment of ICRF2 with the ICRS was made using 138 stable sources common to both ICRF2 and ICRF1. Future maintenance of ICRF2 will be made using a set of 295 new “defining” sources selected on the basis of positional

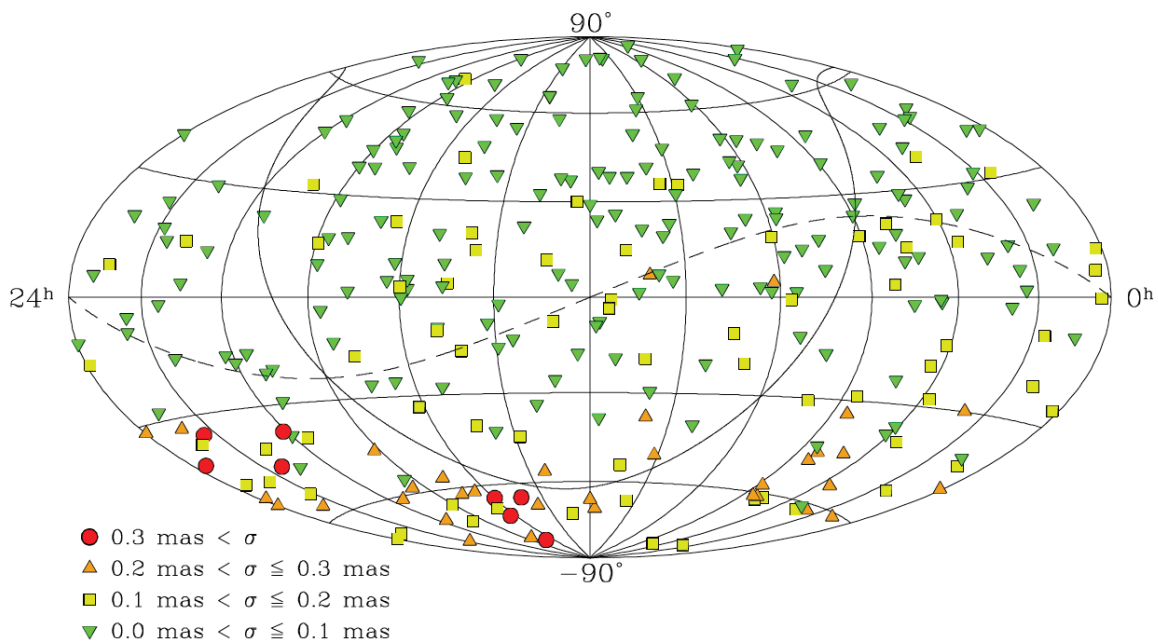


*Fig. 1: The distribution of the 295 new ICRF2 “defining” sources on an Aitoff equal-area projection of the celestial sphere. ICRF2 defining sources were selected on the basis of positional stability and the lack of extensive intrinsic source structure. The dotted line in this figure represents the Galactic equator.*

stability and the lack of extensive intrinsic source structure. The stability of these 295 defining sources, and their more uniform sky distribution eliminates the two largest weaknesses of ICRF1.

On Thursday, August 13, 2009 at the second session of the XXVII General Assembly of the IAU held in Rio de Janeiro, Brazil, members approved, without dissent, Resolution B3 adopting the ICRF2 as the fundamental celestial reference frame as of 1 January 2010.

In the coming decades, there will be significant advances in the area of space-based optical astrometry. Proposed and scheduled missions such as the National Aeronautics and Space Administration’s (NASA) Space Interferometry Mission (SIM-Lite) and the European Space Agency’s (ESA) Gaia mission will achieve astrometric positional accuracies well beyond that presently obtained by any ground-based radio interferometric measurements. In 2008 and 2009, ICRS Centre personnel continued their participation in the NASA SIM mission, through direct involvement in one of the SIM key science projects: Astrophysics of Reference Frame Tie Objects. In addition, ICRS Centre personnel worked on development of a micro-satellite based astrometric mission, called the Joint Milli-Arcsecond Pathfinder Survey (J-MAPS), to produce milliarcsecond level astrometry for all of the bright stars up to 12<sup>th</sup> magnitude (limiting magnitude ~15–16) (see Gaume et al., 2009).

**Monitor source structure to assess astrometric quality**

**VLBA RDV observations and analysis**

Observations of International Celestial Reference Frame (ICRF) sources at radio frequencies of 2.3 GHz and 8.4 GHz using the Very Long Baseline Array (VLBA), together with up to 10 geodetic antennas, continued in 2008 and 2009. These VLBA RDV observations constitute a joint program between the U.S. Naval Observatory (USNO), Goddard Space Flight Center (GSFC) and the National Radio Astronomy Observatory (NRAO) for maintenance of the celestial and terrestrial reference frames. During the calendar year 2008 and 2009, a total of twelve VLBA RDV experiments were observed.

**VLBA high frequency reference frame**

VLBA observations to extend the ICRF to K-band (24 GHz) and Q-band (43 GHz) continued in 2008 and 2009. These observations are part of a joint program between the National Aeronautics and Space Administration, the USNO, the National Radio Astronomy Observatory (NRAO) and Bordeaux Observatory. During 2009 work resulted in two published manuscripts presenting the results of the high frequency reference frame observations (Charlot et al., 2010; Lanyi et al., 2010).

**The Radio Reference Frame Image Database**

The Radio Reference Frame Image Database (RRFID) is a web accessible database of radio frequency images of ICRF sources. The RRFID currently contains 7279 Very Long Baseline Array (VLBA) images of 782 sources at radio frequencies of 2.3 GHz and 8.4 GHz. Additionally, the RRFID contains 1706 images of 282 sources at frequencies of 24~GHz and 43~GHz. The RRFID can be accessed from the Analysis Center web page or directly at <http://rorf.usno.navy.mil/rrfid.shtml>.

**The Bordeaux VLBI Image Database**

The Bordeaux VLBI Image Database (BVID) is a web accessible database of radio frequency images of ICRF sources. The BVID currently contains 1898 Very Long Baseline Array (VLBA) images of 824 sources at radio frequencies of 2.3 GHz and 8.4 GHz. The BVID can be accessed from the Analysis Center web page or directly at <http://www.obs.u-bordeaux1.fr/BVID/>.

**Maintenance of the link to the Hipparcos catalog**

During the reporting period (2008/2009) USNO continued to make progress in the areas of UCAC project (release of UCAC3), the extragalactic link to radio frame sources, URAT, and JMAPS.

UCAC3, the first all-sky catalog of the USNO CCD Astrograph Catalog (UCAC) project was release in August 2009 at the IAU GA and the data are available from CDS. Unfortunately the reductions of the NPM data were not completed in time which lead to preliminary proper motions of stars fainter than about  $R = 13$  for declinations north of  $-30$  deg with significant systematic errors up to about 10 mas/yr (Zacharias et al., 2010a). The final release,

UCAC4, expected in 2011 will fix this and other issues, and also make positions at CCD observing epochs public.

Re-reductions of the Southern Proper Motion (SPM) data could be completed in collaboration with Yale University, leading to very accurate proper motions in UCAC3 for south of  $-30$  deg declination utilizing the SPM first epoch data on the Hipparcos system. Based on the first and second epoch SPM data the SPM4 catalog was created containing about 100 million stars with highly accurate proper motions based on an extragalactic system utilizing galaxies ([www.astro.yale.edu/astrom/spm4cat/spm4.html](http://www.astro.yale.edu/astrom/spm4cat/spm4.html)).

While comparing the original and the 2007 versions of the Hipparcos Catalogue with UCAC and other data, large position differences up to several 100 mas were found for some stars in a random sample of about 1500 stars. These are problem cases related to the short epoch span of Hipparcos observations. All combinations of which catalog is off are seen. Results were presented at a DDA meeting (Zacharias et al., 2009).

Reductions of the deep CCD images taken of extragalactic, compact radio sources during the UCAC project continued, with 1 more observing run reduced. Reviewing the results of several such observing runs, systematic offsets between the optical and radio positions are found far in excess of expected, internal errors for some sources. This could be an issue of the Tycho-2 reference frame itself, or a physical offset of the centers of emission (optical-radio) for some quasars. The effect is on the 30 mas level and preliminary results were presented at the 2009 IAU GA (Zacharias & Zacharias, 2009).

Monitoring a sample of 12 ICRF optical counterparts continued at the 1.55m telescope at NOFS, as well as photometric monitoring for reference frame source selection (Ojha et al., 2009). USNO also participated in the construction of the Large Quasar Reference Frame (LQRF), (Andrei et al., 2009), and the Space Interferometry Mission, SIMLite project (Unwin et al., 2009). In a collaboration with Copenhagen Univ. the Brorfelde Schmidt CCD catalog was published (Zacharias et al., 2010b). It contains accurate positions of 13.7 million stars north of  $+49$  deg declination on the Tycho-2 system and goes deeper than UCAC.

Hardware construction of the USNO Robotic Astrometric Telescope (URAT) continued (Zacharias, Wieder, & Bredthauer, 2009). The mechanical work for the new tube assembly of the 20 cm USNO astrograph “redlens” was completed by the USNO Instrument Shop. Wiring of the mount and work on the electronic interface began. Manufacturing of STA1600B CCD chips (10560 x 10560 pixels) was successful. Delivery of the “4-shooter” camera (4 of these large CCDs plus 3 guide chips) is expected in 2010. For latest progress about the URAT project see:

### 3.5.4 ICRS Centre

<http://www.usno.navy.mil/USNO/astrometry/optical-IR-prod/urat/usno-robotic-astrometric-telescope-urat/>

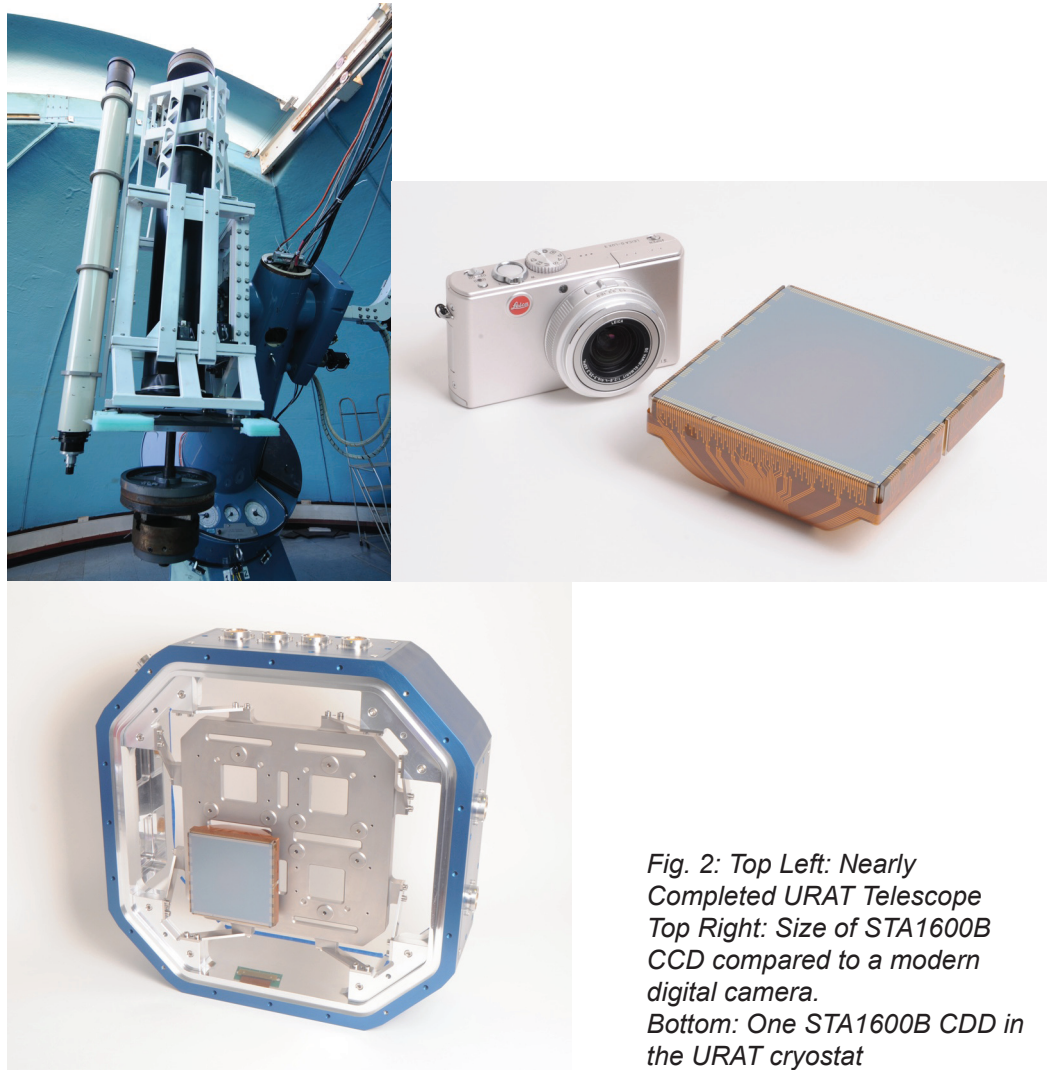


*Fig. 2: Top Left: Nearly Completed URAT Telescope  
Top Right: Size of STA1600B CCD compared to a modern digital camera.  
Bottom: One STA1600B CDD in the URAT cryostat*

### Linking the ICRF to frames at various wavelengths

#### Optical representation of the ICRS

In recent years there was a significant increase of the number of optically bright quasars for which an ICRF related astrometric position can be derived, along with an improvement of the evenness of their sky distribution (Véron-Cetty & Véron, 2006; Souchay et al., 2008). This enabled to build an optical representation of the ICRS, the LQRF (Andrei et al., 2009) formed by 100,165 QSOs all-sky distributed (see next paragraph).

This answers to the requirements such as from micro and macro lensing, binaries, and space density counts, as well as the requirements of space astronomy missions. In particular, for the forthcoming Gaia mission an Initial Quasar Catalogue is being

compiled. The workpackage is formed by A.H. Andrei (ON/MCT, OATo/INAF, OV/UFRJ), C. Barache (SYRTE/OP), D.N. da Silva Neto (UEZO/RJ), F. Taris (SYRTE/OP), G. Bourda (Obs. Bordeaux), J.-F. LeCampion (Obs. Bordeaux), J. Souchay (SYRTE/OP), J.I.B. Camargo1 (ON/MCT), J.J. Pereira Osório (CICGE/FCUP), M. Assafin (OV/UFRJ), P. Charlot (Obs. Bordeaux), R. Vieira Martins (ON/MCT), S. Bouquillon (SYRTE/OP) & S. Anton (CICGE/FCUP). Also A.-M. Gontier (SYRTE/OP) belonged to this workpackage and her absence will be sorrowly felt.

The latest version of the Gaia Initial Quasar Catalogue (GIQC\_III) contains 174,744 sources, divided in 3 categories: defining (full reliability, 123,880 sources), candidate (lacking full confirmation of redshift or magnitude or pointlikeness, 24,229 sources), and other (pending confirmation of two or more characteristics, 26,235 sources). The GIQC\_III includes morphological indexes, as derived from the study of the target's PSF from DSS R, B, and I plates, in comparison with at least 6 well imaged neighbor stars. It also includes the most reliable positions, magnitudes, and redshifts. Figure 3 presents an extract of the GIQC\_III. The catalogue may be consulted on demand to oat1@on.br (A. Andrei).

The morphological indexes were determined from 5x5 arcmin cuts of B, R, I DSS images. At least 6 well imaged are retained as comparison to the quasar's PSF. The IRAF measures SHARP (probing skewness), SROUND (probing roundness), and GROUND (probing normalness) define the indexes. The robustness of the morphological indexes was verified by a trial bench on 1,343 R images for which also the SDSS DR7 images (0.396 arcsec/px) were retrieved. The results show that the PSF analysis reproduces well the SDSS star/galaxy separator and that the DSS plates per-

RA (deg)	DEC (deg)	MAG	z	Rshr	Rsrn	Rgrn	Bshr	Bsrn	Bgrn	Ishr	Isrn	Igrn	Class
0.000000	-0.032778	19.40	1.560										C P
0.002083	-0.450833	20.09	0.250										O F
0.005291	-2.033269	19.29	1.356	0.75	0.10	0.13							D
0.005735	-30.607458	19.18	1.143	0.20	0.01	0.91							D
0.007326	-31.373790	19.74	1.331	0.73	0.44	0.00			1.82	1.14	1.37		D
0.011279	-25.193609	21.56	1.314										O F
0.012178	-35.059062	17.09	0.508	0.59	0.20	0.27			0.39	0.80	0.07		D
0.022792	-27.419533	19.11	1.930	0.12	1.01	0.41							D
0.027500	0.515278	20.37	1.823										D S
0.033333	-63.593333	17.00	0.136										C A
0.034167	0.276389	20.03	1.837										D S
0.038604	15.298477	19.40	1.199	0.92	0.02	0.30	0.36	0.92	0.08	1.11	1.51	1.46	D S
0.039089	13.938450	18.29	2.240	0.59	0.23	0.14	0.63	0.91	0.09	2.07	0.16	1.43	D S

Fig. 3: The first lines of the Gaia Initial Quasar Catalogue – GIQC\_III RA and DEC are self-explanatory. And so is the redshift (z) on the 4th column. MAG is V whenever available, when it is not g, r, or the weighted average of the available colors. It follows 3 groups (from the DSS R, B, and I plates) of 3 PSF estimators (SHARP, SROUND, and GROUND) for which the closer to 0, the more stellar-like is the QSO PSF (in the local photometric standard). The first Class column is Defining, Candidate, or Other. The second Class column is SDSS source (for Ds); ICRF source, optically point-like AGN, or Poor observational history (for Cs); Empty field, low precision Radio position, Unreliable detection, or optically Faint (for Os).

### 3.5.4 ICRS Centre

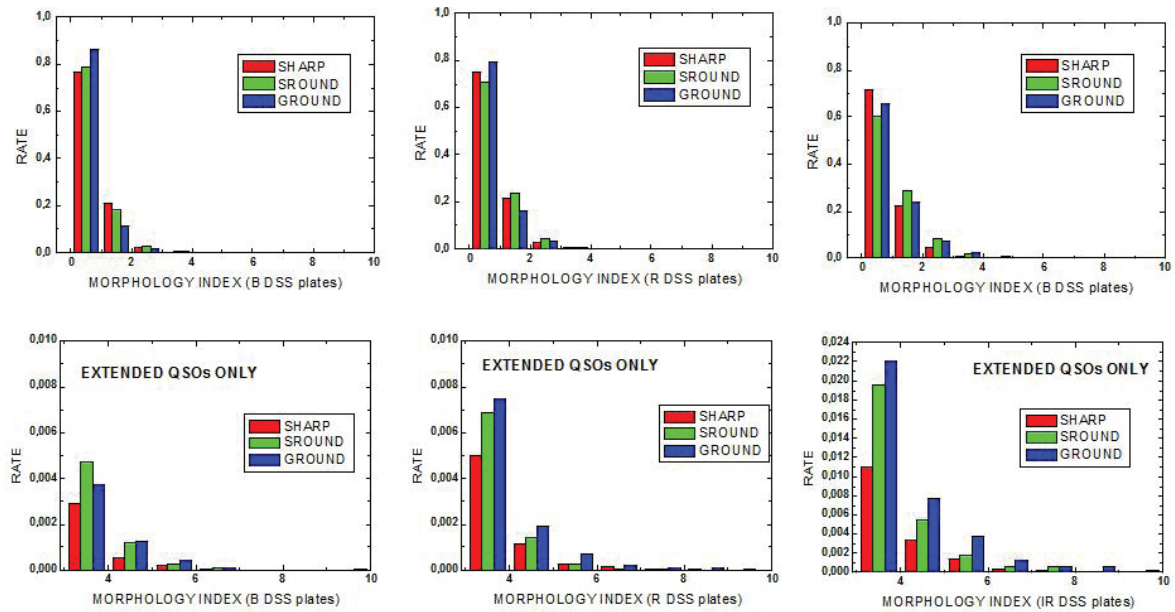


*Fig. 4: Histograms of the morphological indexes are shown on the upper row. The second row zooms the histograms into the region of non-pointlikeness. It is evident that the degree of non-pointlikeness varies along the spectrum. The bluer the QSO is looked to, the deeper into the power force it is perused, and the more pointlike it looks. Notice that the atmosphere transparency works right against this.*

form much alike to the SDSS frames. The excess (rate of objects beyond  $2\sigma$ ) of non-stellar quasars is significant as given by all the indicators, on both the DSS2 and DR7 images, measured either against the field stars or the SDSS classified stars.

#### Construction of the LQRF

The large number, and all sky repartition of quasars from different surveys combined with their presence in large, deep astrometric catalogs, enabled to build an optical materialization of the ICRS (International Celestial Reference System) following its defining principles, namely, kinematically non-rotating with respect to the ensemble of distant extragalactic objects, aligned to the mean equator and dynamical equinox of J2000, and realized by a list of adopted coordinates of extragalactic sources.

The LQRF (Large Quasar Reference Frame) (Andrei et al., 2009) was built with the care of avoiding wrong matches of its constituents quasars, of homogenizing the astrometry from the different catalogs and lists from which the constituent quasars are gathered, and of attaining the milli-arcsecond global alignment to the ICRF (International Celestial Reference Frame), as well as typical individual source position accuracies even to better than 100 mas.

Starting from the updated and presumably complete LQAC (Large Quasar Astrometric Catalog) (Souhay et al., 2009) list

of QSOs, initial optical positions for those quasars were found in the USNO B1.0 and GSC2.3 catalogs, and from the SDSS Data Release 5. The initial positions were next placed onto UCAC2 based reference frames, followed by an alignment to the ICRF, as well as to the most precise sources from the VLBA calibrator list and from the VLA calibrator list, when reliable optical counterparts exist. Finally the LQRF axes were inspected through spherical harmonics, contemplating right ascension, declination and magnitude terms. Thus a method akin to the enlargement of the ICRF2 was used.

The LQRF contains 100,165 quasars, well represented on all-sky basis, from  $-83.5^\circ$  to  $+88.5^\circ$  of declination, and with 10 arcmin as the average distance between adjacent elements (Fig 5). The global alignment to the ICRF is of 1.5 mas (Fig. 6), and the individual position accuracies are represented by a Poisson distribution peaking at 139 mas on right ascension and at 130 mas on declination (Fig. 7). As a by product, significant equatorial corrections appear for all the used quasar catalogs but the SDSS DR5.

The LQRF contains J2000 referred equatorial coordinates, and is completed by redshift and photometry information from the LQAC. It is aimed to be an astrometric frame, but it is also the basis for the Gaia mission initial quasars' list, and can be used as a test bench for quasars' space distribution and luminosity function studies. The LQRF is meant to be updated after the release of new quasar identifications and newer versions of the used astrometric frames.

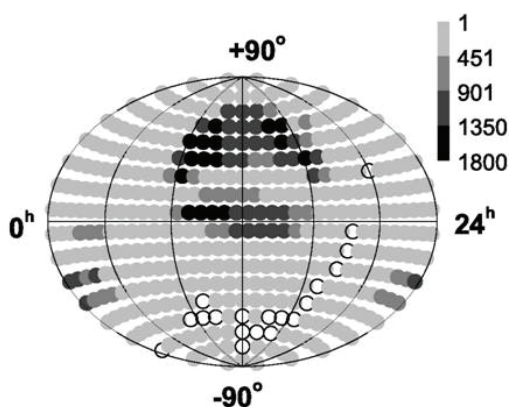


Fig. 5: Sky density of the LQRF. The counts are in bins of  $10^\circ$ . The void regions shown by white circles are in the galactic plane. The densest patches lie on the SDSS region.

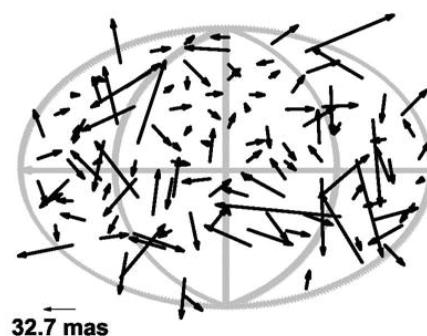
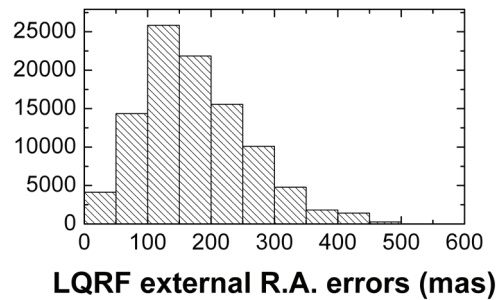
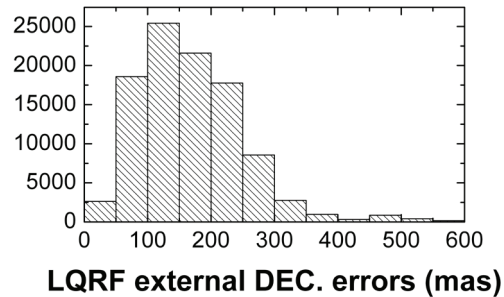


Fig. 6: Vectorial distribution of the systematic deviations (north up east right of the LQRF to the ICRF, bins of  $10^\circ$ ). The average value is 32.7 mas, graphically represented by the off map arrow.



*Fig. 7: Distribution of the external errors assigned to the right ascension and declination for the J2000 positions of the LQRF sources. The distributions can be reckoned as Poisson distributions peaking at 139 mas on right ascension and at 130 mas on declination.*



#### **Data bank of optical images of QSOs**

In order to provide the basis for independent optical astrometry and morphology studies of quasars as the fiducial points of materialization of the ICRS, a data bank of images has been compiled during 2008. The images comprise the first and second realizations of the DSS (Digitized Sky Survey), as well as the available recent, deeper CCD frames (e.g., from the SDSS – Sloan Digital Sky Survey).

A first extract of the data bank was produced over 1,343 objects belonging to the SDSS (Fig. 8). For these, the SDSS images on filters g, r, and i, and the DSS II images on filters B, R, and I were retrieved and their morphology was analyzed. Parameters of sharpness, roundness, and normalness were derived from the plate and CCD images, and compared against the neighbor stellar sample.

The use of those parameters allowed us to separate the stellar and non-stellar populations, with performance well adjusted (up to 88 %) to that of the SDSS. Among the QSO's an excess of about 30% of non-pointlike objects was found, indicating the signature of the host galaxy (Fig. 9).

The data bank will be made available for browsing through the IERS-ICRS site, and mirror sites from the associated institutes: SYRTE at Paris Observatory, Centro de Investigação em Ciências Geo-Espaciais/FCUP (Portugal), and Observatorio Nacional/MCT (Brasil).

Fig. 8: Sky distribution of the 1,343 trial bench sample. It includes the extreme magnitudes, colors, and redshift objects, along with a representative DR7 population.

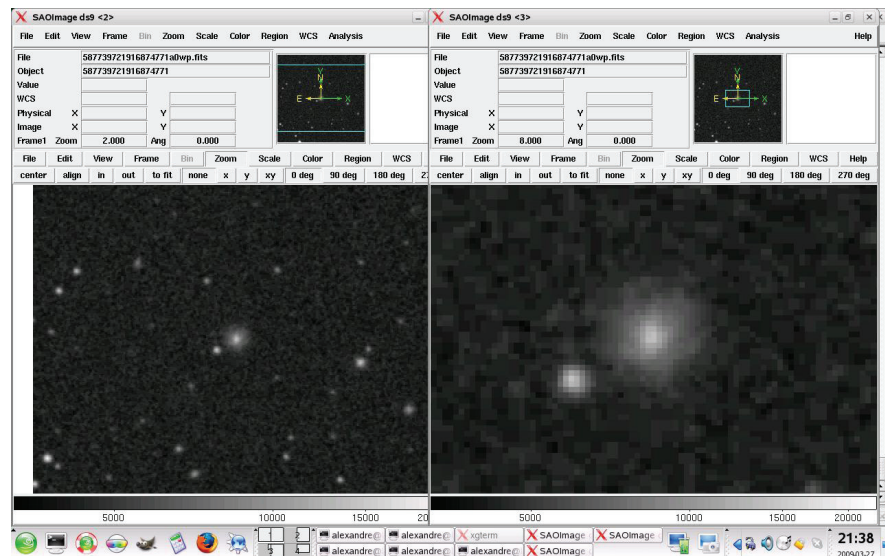


Fig. 9: Example image of QSO DR7 587739721916874771 from the DSS II red plate. The zoomed DS9 window on the right leaves evident an elliptical galaxy underneath the QSO.

### Maintenance of the link to the solar system dynamical reference frame using Lunar Laser Ranging analyses

Analysis of the Lunar Laser Ranging (LLR) provides scientific results in various domains (astronomy, gravitational physics, geodynamics, selenophysics). The LLR observations contribute also to the positioning of the dynamical reference frame with respect to ICRS.

At the lunar analysis centre of Paris Observatory (SYRTE laboratory), we define the dynamical reference frame of the solar system as the dynamical mean ecliptic and equinox J2000 related to the orbit of the Moon given by the lunar ephemerides of the solution ELP (Chapront-Touzé et al., 1997).

The LLR data (normal points) consist in measurements of the round-trip travel time of the light between a terrestrial station and a lunar reflector. According to a recent inventory of LLR observations collected since 1969 (Francou et al., 2009), we have gathered more than 18000 LLR normal points provided by four stations: Mc-

Donald (Texas) 1969–2008, OCA (France) 1984–2005, Haleakala (Hawaii) 1984–1990, Apache Point (New Mexico) 2006–2008.

The analyses of the differences between the LLR observations and the values computed with ELP give post-fit residuals around 300 picoseconds for the round-trip travel time of the light, that is to say less than 5 cm for the distance station-reflector.

The position of the dynamical mean ecliptic with respect to ICRS (J2000 epoch) resulting from LLR analyses is defined by the two angles:

- $\varepsilon^{(\text{ICRS})}$ , the inclination of the dynamical mean ecliptic to the equator of ICRS,
- $\varphi^{(\text{ICRS})}$ , the angle between the origin  $\alpha^{(\text{ICRS})}$  of right ascensions on the equator of ICRS and the ascending node  $\gamma_1^{(\text{ICRS})}$  of the dynamical mean ecliptic on the equator of ICRS.

Different evaluations of  $\varepsilon^{(\text{ICRS})}$  and  $\varphi^{(\text{ICRS})}$  made for various time intervals of LLR observations and using different models of precession-nutation, give very close results (Table 3).

Table 3: Evaluation of  $\varepsilon$  and  $\varphi$  by different authors.

Authors	Time intervals	$\varepsilon^{(\text{ICRS})}$	$\varphi^{(\text{ICRS})}$
Chapront J. et al. (2002)	1969–2001	23°26'21.41100"±0.00005"	−0.05542"±0.00011"
Zerhouni W. et al. (2007)	1969–2006	23°26'21.41081"±0.00009"	−0.05538"±0.00009"
Francou G. et al. (2009)	1969–2008	23°26'21.41125"±0.00009"	−0.05543"±0.00009"

The uncertainties mentioned in Table 3 being formal uncertainties resulting from the least square fitting, the final values for these angles are fixed as follows:

$$\varepsilon^{(\text{ICRS})} = 23^{\circ}26'21.411''$$

$$\varphi^{(\text{ICRS})} = \alpha^{(\text{ICRS})}\gamma_1^{(\text{ICRS})} = -0.055 \text{ mas}$$

Simultaneously to the determination of the position of the dynamical reference frame, the LLR analyses have also allowed us to determine other parameters (Bouquillon et al., 2005; Chapront et al., 2006; Zerhouni et al., 2008) and to perform adjustments of the motions of Moon (Chapront et al., 2003; Manche et al., 2007).

### Maintenance of the link to the solar system dynamical reference frame using Pulsar Timing analyses

In 2008, activities related to VLBI observations of millisecond pulsars (PSR) and the link between dynamical reference frames and ICRF based on PSR observations have been maintained and amplified. A PhD student began his thesis in September 2008 at the Besançon observatory on the use of PSRs in reference frame tie and detection of gravitational waves.

**Rotation between planetary ephemerides: DE200, DE405 and INPOP06**

In association with the Nançay Radio Telescope (NRT) and the LPCE (CNRS/University of Orléans) and in the frame of the 4-years french plan “Systèmes de référence: Raccordement de l’ICRF et du système de référence dynamique d’INPOP (Reference Systems linking the ICRF to the Dynamical System INPOP)”, we developed this new investigation based on the use of millisecond pulsar timing (TOA) obtained at the NRT (Cognard, 2006). The tempo2 software (Hobbs et al., 2006) was used to proceed the TOA observations.

Coordinates estimated in using pulsar timing data (TOA) are expressed in the reference frame of the planetary ephemerides used in the reduction process. By considering only PSRs TOA, rotation matrices between dynamical frames can be estimated. The differences in  $(\alpha_{\text{TOA}}, \delta_{\text{TOA}})$  induced by the use in the reduction procedure of different planetary ephemerides (DE200, DE405 and INPOP06) indicate small rotations of the dynamical frames of the planetary ephemerides. In Table 4, one can find the PSR coordinates used to compute the rotation matrices  $W$  between DE405 and DE200 in one hand and DE405 and INPOP06 in the other hand. We find in mas  $W[\text{DE405–DE200}] = [0.4 \pm 3, 11 \pm 4, 13 \pm 3]$ . This matrix is close to the one deduced from estimations done by (Standish 1998a, 1998b) at J2000,  $S[\text{DE405–DE200}] = [1.3, 13.7, 10.3]$ . Between DE405 and INPOP06, we obtain  $W[\text{DE405–INPOP}] = [1.7 \pm 0.5, 0.55 \pm 0.05, 1.0 \pm 0.1]$ . These latest rotations between DE405 and INPOP06 are statistically significant but they remain below the 1 to 10 mas uncertainties of the VLBI tracking observations of spacecrafts used to link the dynamical frame of DE or INPOP to ICRF.

**Rotation between ICRF and planetary ephemerides**

An independent way to establish a link between a dynamical reference frame built on the basis of a planetary ephemeris and ICRF, is to use VLBI observations of millisecond pulsars combined with pulsar timing.

A new proposal of VLBI observations of 3 PSRs was done at the European VLBI Network (EVN) for the first semester of 2009. The rate priority being 1.6, the proposal was accepted for observation but not scheduled yet. A new proposal for the same objects was then again proposed for the first semester of 2010. Besides, new VLBI observations of PSRs have been done by other teams: Chatterjee et al. in US and Deller et al. in Australia. Based on these new positions and in using radio pulsar timing (TOA) performed at the Nançay radio telescope (NRT), we have been able to perform new link between DE405, INPOP06 and ICRF.

We note  $(\alpha_{\text{TOA}}, \delta_{\text{TOA}})$  the pulsar coordinates obtained with pulsar timing and expressed in the reference frame of the planetary ephemerides used in the reduction process. Besides, VLBI observations of the same pulsars done in using ICRF sources as

calibration sources are given directly in ICRF. Let us note  $(\alpha_{\text{VLBI}}, \delta_{\text{VLBI}})$  the coordinates of the pulsars obtained with VLBI. The comparisons between these two sets of coordinates  $(\alpha_{\text{TOA}}, \delta_{\text{TOA}})$  and  $(\alpha_{\text{VLBI}}, \delta_{\text{VLBI}})$  give then the rotations between the ICRF and the dynamical reference frame of the planetary ephemerides as well as possible drift of the dynamical reference frame if the comparisons are extended in time.

To obtain high accurate determinations, we estimate the rotation matrix in using PSRs observations presented in Table 4 and with TOA uncertainties in positions of about 1 mas. This means that we use B1937+21 and J1713+0747. As it is shown in Table 4, the data from NRT were not sufficient to obtain a good astrometry based on TOA of 0139+5814, 1300+1240 and 0454+5543.

In using the two pulsars B1937+21 and J1713+0747, we obtain in mas the rotation matrix  $M$  at J2000  $M[\text{INPOP-ICRF}] = [9 \pm 5, -3 \pm 1, -4 \pm 5]$ . This rotation is statistically significant but at the limit of accuracy of the present observations used to link planetary ephemerides to ICRF. We deduce the matrix  $M[\text{DE405-ICRF}] = [11 \pm 6, -2.5 \pm 11, -3 \pm 5]$  at J2000. We would expect smaller values (Standish 1998b). This can be seen as a systematic induced by the fact that we only use two pulsars to make the link. The link must be extended to other pulsars by adding to the NRT TOA data TOA obtained by other observatories. By adding new sets of observations, we decorrelate instrumental errors and improve the astrometric accuracy.

*Table 4: Candidates of pulsars for reference frame link: Column 1 gives the name of the PSR, Columns 2 and 3 give the J2000 equatorial coordinates. Column 4 gives the RMS of TOA residuals obtained with the NRT observations and proceeded with tempo2 software. Columns 5 and 6 give the astrometric accuracies in positions obtained with NRT TOA and tempo2. The last column indicates the reference of the VLBI observations: C09 stands for (Chatterjee et al. 2009), NB98 for (Nunes and Bartel, 1998), B96 for (Bartel et al., 1996) and P94 for (Petit, 1994).*

	RA [hhmmss.s]	DE [ddmmss.s]	RMS TOA [ $\mu$ s]	$\sigma \alpha$ [mas]	$\sigma \delta$ [mas]	VLBI
J0139+5814	01 39 19.77	58 14 31.8	62	800	70	C09
J0437-4515	04:37:15.749	-47:15:08.23	0.9	0.16	0.14	
J1909-3744	19:09:47.437	-37:44:14.32	0.3	0.1	0.2	
J1824-2452	18:24:32.00	-24:52:10.69	6	0.3	0.4	
J1300+1240	01 39 19.77	58 14 31.8	9	50	118	NB98
B1937+21	19 39 38.55	21 24 59.1	0.3	0.1	1	B96, P94
J1713+0747	17 13 49.52	07 47 37.5	0.2	2	1	C09
J1136+1551	11 36 03.30	15 51 00.7	125	19	35	
J1744-1134	17:44:29.401	-11:34:54.64	0.9	0.4	0.9	
J0454+5543	04 54 07.75	55 43 41.4	87	130	60	C09

**Staff** Souchay, Jean, Director (OP)  
Gaume, Ralph, Co-director (USNO)

Andrei, Alexandre, Assoc. Astronomer (OP, Obs. Nat. Rio, Brasil)  
Arias, E. Felicitas, Assoc. Astronomer (BIPM / OP)  
Barache, Christophe, Engineer (OP)  
Boboltz, David, Astronomer (USNO)  
Bouquillon, Sébastien, Astronomer (OP)  
Chapront, Jean, Astronomer (OP)  
Chapront-Touzé, Michelle Astronomer (OP)  
Fey, Alan, Astronomer (USNO)  
Fienga, Agnès, (Observatoire de Besançon)  
Francou, Gérard, Astronomer (OP)  
Gontier, Anne-Marie, Astronomer (OP, deceased in 2010)  
Lambert, Sébastien, Astronomer (OP)  
Le Poncin-Lafitte, Christophe, Post-doc (OP)  
Taris, François, Technician (OP)  
Zacharias, Norbert, Astronomer (USNO)  
Zerhouni, Wassila (OP)

**References** Andrei, A.H., Souchay, J., Zacharias, N., Smart, R.L., Vieira Martins, R., da Silva Neto, D.N., Camargo, J.I.B., Assafin, M., Barache, C., Bouquillon, S., Penna, J.L., Taris, F., 2009, A&A (accepted)

Bartel, N., et al., 1996, *Astron. J.*, 112, 1690

Charlot, P., Boboltz, D. A., Fey, A. L., Fomalont, E. B., Geldzahler, B. J., Gordon, D., Jacobs, C. S., Lanyi, G. E., Ma, C., Naudet, C. J., Romney, J. D., Sovers, O. J., Zhang, L. D. ,2010, *Astron. J.*, 139, 1713

Chatterjee, S., et al., 2009, arXiv:0901.1436

Cognard, I., 2006, Atelier 'Pulsars : théories et observations', IAP Paris, 16–17 janvier 2006

Feissel-Vernier, M., Ma, C., Gontier, A.-M., & Barache, C., 2006, Analysis issues in the maintenance of the ICRF axes, A&A, 452, 1107

Fey, A. L., Gordon, D. & Jacobs, C. S., 2009, The Second Realization of the International Celestial Reference Frame by Very Long Baseline Interferometry, Presented on behalf of the IERS / IVS Working Group, Alan Fey, David Gordon, and Christopher S. Jacobs (eds.). (IERS Technical Note ; 35) Frankfurt am Main: Verlag des Bundesamts für Kartographie und Geodäsie. 204 p., ISBN 3-89888-918-6 (print version)

Fey, A.L., Ma, C., Arias, E.F., Charlot, P., Feissel-Vernier, M., Gontier, A.-M., Jacobs, C.S., Li, J., & MacMillan, D.S. ,2004, The Second Extension of the International Celestial Reference Frame: ICRF-EXT.1, *Astron. J.*, 127, 3785

### 3.5.4 ICRS Centre

- Gaume, R., Dorland, B., Hennessy, G., Dudik, R., Bartlett, J., Dugan, N., Zacharias, N., Johnston, K., Barrett, P., Makarov, V., 2009, The Joint Milli-Arcsecond Pathfinder Survey (J-MAPS) Mission, 213th AAS meeting, Long Beach, California, January 2009, Bull. Amer. Astron. Soc. 41, No. 1, 344, #451.01
- Hobbs, G. B., et al., 2006, MNRAS, 369, 655
- Lanyi, G. E., Boboltz, D. A., Charlot, P., Fey, A. L., Fomalont, E. B., Geldzahler, B. J., Gordon, D., Jacobs, C. S., Ma, C., Naudet, C. J., Romney, J. D., Sovers, O. J., Zhang, L. D., 2010, Astron. J., 139, 1695
- Ma, C., Arias, E.F., Eubanks, T.M., Fey, A.L., Gontier, A.-M., Jacobs, C.S., Sovers, O.J., Archinal, B.A., Charlot, P., 1998, The International Celestial Reference Frame as realized by very long baseline interferometry, Astron. J., 116, 516
- Nunes, N. V., Bartel, N., 1998, IAU Colloquium 164
- Petit, G., 1994, Ph.D. thesis, Observatoire de Paris (in French)
- Souchay, J., Andrei, A.H., Barache, C., Bouquillon, S., Suchet, D., Baudin, M., Gontier, A.-M., Lambert, S., Le Poncin-Lafitte, C., Taris, F., Arias F.E., 2008, A&A, 485, 299
- Standish, E. M., 1998a, IOM 312-F
- Standish, E. M., 1998b, IV International Workshop on Positional Astronomy and Celestial Mechanics
- Unwin, S. et al., 2009, SIM Lite Astrometric Observatory, NASA, JPL
- Zacharias, M.I. & Zacharias, N., 2009, Significant radio-optical reference frame offsets from CTIO data, Division I poster paper IAU GA 2009; abstract in upcoming Reports
- Zacharias, N., Wieder, G., & Bredthauer, R., 2009, USNO Robotic Astrometric Telescope (URAT) phase 1 = U-mouse, 213th AAS meeting, Long Beach, California, January 2009, Bull. Amer. Astron. Soc. 41, No. 1, 421, #470.11
- Zacharias, N., Finch, C., Wycoff, G., Hartkopf, W., 2009, Improving Hipparcos Proper Motions with UCAC, DDA meeting 2009, Virginia Beach, Bull. Amer. Astron. Soc., 41, No.2, p. 910, abstract #16.03
- Zacharias, N., Finch, C., Girard, T., Hambly, N., Wycoff, G., Zacharias, M.I., et al., 2010a, The Third US Naval Observatory CCD Astrograph Catalog (UCAC3), Astron. J., 139, 2184–2199
- Zacharias, N. Einicke, O.H., Augustesen, K., Clausen, J.V., Finch, C., Hoeg, E., Wycoff, G.L., 2010b, Brorfelde Schmidt CCD catalog, Astron. J., 140, 652

*Ralph Gaume, Jean Souchay, Alexandre Andrei,  
E. Felicitas Arias, Christophe Barache, David Boboltz,  
Sébastien Bouquillon, Jean Chapront, Alan Fey, Agnès Fienga,  
Gérard Francou, Sébastien Lambert, Christophe Le Poncin-  
Lafitte, François Taris, Norbert Zacharias*